HHS Public Access

Author manuscript

Nature. Author manuscript; available in PMC 2012 June 22.

Published in final edited form as:

Nature. ; 480(7378): 570–573. doi:10.1038/nature10622.

Intermediates in the Transformation of Phosphonates to Phosphate by Bacteria

Siddhesh S. Kamat, **Howard J. Williams**, and **Frank M. Raushel**

Department of Chemistry, P.O. Box 30012, Texas A&M University, College Station, Texas 77843 USA

Phosphorus is an essential element for all forms of life. In living systems, phosphorus is an integral component of nucleic acids, carbohydrates, and phospholipids where it is incorporated as a derivative of phosphate. However, most gram-negative bacteria have the capability of utilizing phosphonates as a nutritional source of phosphorus under conditions of phosphate starvation[1]. In these organisms methyl phosphonate is converted to phosphate and methane (equation (**1**)). In a formal sense this transformation is a hydrolytic cleavage of a carbon-phosphorus bond but a general enzymatic mechanism for the activation and conversion of alkylphosphonates to phosphate and an alkane has not been elucidated despite much effort for more than two decades. The actual mechanism for C-P bond cleavage is likely to be a radical-based transformation[2]. In *Escherichia coli* the catalytic machinery for the C-P lyase reaction has been localized to the *phn* gene cluster[1]. This operon consists of 14 genes denoted as *phnCDEFGHIJKLMNOP*. Genetic and biochemical experiments have demonstrated that the *phnGHIJKLM* genes encode proteins that are essential for the conversion of phosphonates to phosphate and that the other proteins have auxiliary functions[1,3–6]. There are no functional annotations for any of the seven proteins considered essential for C-P bond cleavage. Here we show that methylphosphonate reacts with MgATP to form α-D-ribose-1-methylphosphonate-5-triphosphate (RPnTP) and adenine. The triphosphate moiety of RPnTP is hydrolyzed to pyrophosphate and α-D-ribose-1-methylphosphonate-5-phosphate (PRPn). The carbon-phosphorus bond of PRPn is subsequently cleaved via a radical-based reaction to α-D-ribose-1,2-cyclic-phosphate-5-phosphate (PRcP) and methane in the presence of *S*-adenosyl-L-methionine. Substantial quantities of phosphonates are produced worldwide for industrial processes, detergents, herbicides and pharmaceuticals [7–9]. The elucidation of the chemical steps for the biodegradation of alkylphosphonates has unveiled for the first time how these compounds can be metabolized and recycled to phosphate.

Correspondence should be addressed to F.M.R (raushel@tamu.edu).

Supplementary Information is linked to the online version of the paper at www.nature.com/nature.

Author Contributions S.S.K., H.J.W. and F.M.R. designed the experiments. S.S.K. and H.J.W. performed the experiments. S.S.K., H.J.W. and F.M.R. wrote the manuscript.

Author Information The authors declare no competing financial interests.

The genes for the seven essential proteins encoded by the *phnGHIJKLM* gene cluster were cloned, expressed in *E. coli* and the proteins purified to homogeneity. PhnI, PhnJ, PhnK and PhnL were purified as N-terminal glutathione *S*-transferase (GST) fusion proteins. PhnG, PhnH and PhnM were purified without a GST-tag. Previous experiments have hinted of a ribose intermediate for the esterification of phosphonate substrates prior to conversion to phosphate[10,11]. Since PhnI showed a distant relationship to enzymes that are functionally annotated as nucleosidases[12], we incubated this protein with a small focused library of potential ribose donors. The liberation of the free base was followed spectrophotometrically at 240–350 nm in the presence of coupling enzymes that are capable of detecting the formation of adenine[13], guanine[14], cytosine[15] or xanthine[16]. The best substrates for PhnI are GTP and ATP (k_{cat}/K_m = 8.3 × 10^4 M^{-1} s^{-1} and 1.3 × 10^4 M^{-1} s^{-1}, respectively). The products are D-ribose-5-triphosphate (RTP) and the free base as shown for ATP in equation (**2**). The kinetic constants for the nucleosidase activity of PhnI with GTP and ATP are listed in Table S1. The structure of RTP was identified by ^{31}P-NMR spectroscopy and further confirmed by multi-dimensional NMR.

The formation of RTP from either ATP or GTP did not appear to be a productive pathway for the transformation of phosphonates to phosphate. We therefore incubated phosphate and phosphonate derivatives with MgATP in the presence of PhnI to determine if any of these compounds could displace adenine. RTP and adenine were the only products formed in the presence of either phosphate or phosphonate derivatives. There were no changes in the reaction products whether we used the GST-tagged PhnI in the presence or absence of Factor Xa[17]. Since it was previously postulated that the C-P lyase reaction may involve a multi-protein complex[3,18], additional proteins were added to the reaction mixture. PhnG, PhnH, PhnK and PhnL were incubated together with PhnI, MgATP and methylphosphonate but no new products were detected other than RTP and adenine. Since PhnI, PhnK and PhnL were all GST-fusion proteins, Factor-Xa was added to the reaction mixture for *in situ* cleavage of the GST-tags. With the addition of Factor-Xa, a new resonance was observed by ^{31}P NMR spectroscopy at 17.8 ppm as shown in Figure 1a. NMR spectra are consistent with the formation of α-D-ribose-1-methylphosphonate-5-triphosphate (RPnTP) as shown in equation (**3**).

To determine whether all of the proteins are required for this transformation, each protein was removed individually from the reaction mixture. The only protein that could be removed was PhnK. Thus, PhnI, in the presence of PhnG, PhnH, and PhnL, is required for catalyzing the nucleophilic attack of methylphosphonate on the anomeric carbon of MgATP to form adenine and RPnTP. The kinetic constants for the reaction of methylphosphonate with ATP (k_{cat}/K_m = 3.5 × 10^5 M^{-1} s^{-1}) and GTP (k_{cat}/K_m = 3.4 × 10^5 M^{-1} s^{-1}) in the presence of PhnI, PhnG, PhnH and PhnL are presented in Table S1. It must be noted that these proteins begin to precipitate after removal of the GST-tags and thus the kinetic constants are not definitive. No reaction was observed with the fusion proteins and the GST-tags must be removed *in situ*. The stoichiometry of the four proteins required for complex formation and the individual functions of PhnG, PhnH and PhnL are uncertain.

Previous studies have suggested α-D-ribose-1-phosphonate-5-phosphate (PRPn) as a potential intermediate in the conversion of alkylphosphonates to phosphate by *E. coli*[6,10,11].

Hence, it was rational to assume that one of the proteins in the *phn* operon would catalyze the hydrolysis of the β- and γ-phosphoryl groups from RPnTP. PhnM was the prime candidate for this reaction since this protein is a member of the amidohydrolase superfamily and members of this superfamily are known to catalyze hydrolytic reactions at carbon and phosphorus centers[19]. PhnM was incubated with RPnTP in the presence of $MgCl_2$ and $ZnCl_2$. The changes in the ^{31}P NMR spectrum are shown in Figure 1b. NMR spectra are consistent with the formation of α-D-ribose-1-methylphosphonate-5-phosphate and pyrophosphate as the major products. D-Ribose-5-diphosphate (RDP) and D-ribose-5-triphosphate are also substrates for PhnM. When the hydrolysis reaction of RTP catalyzed by PhnM was conducted in oxygen-18 labeled water, the oxygen-18 was found exclusively in D-ribose-5-phosphate and not in pyrophosphate. Therefore, water attacks the α-phosphoryl group of RTP rather than the β-phosphoryl group. The reaction catalyzed by PhnM with RPnTP is presented in equation (**4**). The kinetic constants for the hydrolysis of RPnTP, RTP, and RDP by PhnM are provided in Table S1. RPnTP ($k_{cat}/K_m = 1.1 \times 10^5$ M^{-1} s^{-1}) was the best substrate for PhnM and the kinetic constants did not change for the hydrolysis of RPnTP when PhnG, PhnH, PhnI, PhnK, PhnL and Factor-Xa were added to the assay mixture.

The deletion of *phnJ* from *E. coli* led to the identification of α-D-ribose-1-methylphosphonate (RPn) in the growth medium and this has led to the prediction that PRPn is the ultimate substrate for the actual C-P lyase reaction[6]. This conjecture is consistent with our results since we can synthesize this compound from ATP and methylphosphonate by the combined actions of PhnI, PhnG, PhnH, PhnL and PhnM. Of the remaining two enzymes in the *phn* operon, the most likely protein to catalyze the actual carbon-phosphorus bond cleavage is PhnJ. This enzyme has four conserved cysteine residues with a spacing of $Cx_2Cx_{21}Cx_5C$ that could form part of an iron-sulfur cluster[12]. The cleavage of PRPn to PRcP is assumed to involve a radical mechanism and such reactions can be catalyzed by radical SAM enzymes. These enzymes utilize a [4Fe-4S]-cluster and *S*-adenosyl-L-methionine (SAM) to catalyze radical reactions and/or rearrangements[20]. The radical SAM superfamily was originally thought to have a highly conserved Cx_3Cx_2C motif as a signature for harboring the [4Fe-4S]-cluster[20] but with the successful reconstitutions of ThiC[21], HmdA[22] and Dph2[23], a more diverse combination of conserved cysteine residues can function for the assembly of the [4Fe-4S]-cluster. If PhnJ incorporates a [4Fe-4S]-cluster, it is not clear as to which of the four cysteine residues are required.

The as-purified GST-PhnJ fusion protein was blackish in color. ICP-MS of this protein demonstrated the binding of 2.2 ± 0.2 equivalents of iron per PhnJ monomer. The aerobically purified protein was made anaerobic in a glove box by bubbling argon through the protein solution and then allowed to equilibrate for four hours. Reconstitution of the [4Fe-4S]-cluster was initiated by the slow anaerobic addition of a 50-fold excess of $FeSO_4$ and Na_2S. The protein with the reconstituted iron-sulfur cluster has a reddish-brown color. The UV-visible absorption spectrum of PhnJ, reconstituted with iron and sulfide, has a broad absorption band centered at 403 nm that is indicative of a $[4Fe\text{-}4S]^{2+}$ cluster (Figure 2)[20–23]. The absorption band disappears upon addition of 1 mM dithionite (Figure 2), suggesting the

reduction of the $[4Fe\text{-}4S]^{2+}$ cluster to the $[4Fe\text{-}4S]^{1+}$ species, which is the active form for most radical SAM enzymes[20–23].

There are two compounds that are potential substrates for cleavage by PhnJ of the C-P phosphonate bond: PRPn and RPnTP. Both of these compounds were incubated with 125 μM PhnJ that was previously reconstituted with a [4Fe-4S]-cluster, 2 mM SAM and 1 mM dithionite, anaerobically at pH 6.8. The reactions were analyzed by ^{31}P NMR spectroscopy but there was no change in the NMR spectrum for either substrate. When the reaction was supplemented with Factor-Xa, no change in the ^{31}P NMR spectrum was observed with RPnTP, but a new resonance appeared at 16.2 ppm when PRPn was used as a substrate (Figure 1c). The increase in the resonance at 16.2 ppm correlated with a decrease in the phosphonate resonance of PRPn at 16.6 ppm. The new resonance splits into a triplet in the ^{1}H-coupled ^{31}P spectrum (inset to Figure 1c) demonstrating that the product is no longer a methyl phosphonate. The new resonance is consistent with a cyclic phosphate and the proton coupling constant of 21 Hz indicates that the phosphate moiety of the product is esterified to the hydroxyl groups attached to C1 and C2 of the ribose. Thus, PhnJ requires a reduced [4Fe-4S]-cluster and SAM to catalyze the formation of αD-ribose-1,2-cyclic phosphate-5-phosphate (PRcP) from PRPn. The overall reaction is illustrated in equation (**5**). There was no reaction in the absence of added SAM.

Gas chromatography (GC) and mass spectrometry were used to confirm the formation of methane. The [4Fe-4S]-cluster reconstituted PhnJ was incubated with 2 mM SAM, 1 mM dithionite, 5 mM PRPn, and Factor-Xa in a sealed tube for 5 hours. Gas chromatographic analysis of the headspace above the liquid showed a single peak that co-eluted with a methane standard (Figure S2). The formation of methane was confirmed by coupling the output of the GC to a mass spectrometer and detection of a mass of 16. Thus, the two products formed from the action of PhnJ on PRPn are methane and PRcP. We were unable to detect the formation of methanol or formaldehyde in the reaction mixture.

The addition of SAM, dithionite, PhnJ, and Factor-Xa were required for the formation of PRcP and methane from the $[4Fe\text{-}4S]^{2+}$ reconstituted PhnJ. To determine the fate of SAM during the reaction, HPLC and amino acid analysis were employed. HPLC showed the formation of 5′-deoxyadenosine and amino acid analysis confirmed the formation of methionine. These products were only formed when PhnJ (with a reconstituted iron-sulfur center), Factor-Xa, SAM, dithionite and PRPn were added to the reaction mixture. The omission of any one of the above components resulted in no formation of 5′-deoxyadenosine (Figure S3). The concentration of PRcP and methane formed in the presence of reconstituted PhnJ and SAM showed that 1–4 turnovers of product were formed per PhnJ. The small number of turnovers per enzyme may reflect the poor solubility of PhnJ after proteolytic cleavage of the N-terminal GST-fusion tag and the instability of the [4Fe-4S]-cluster. A working model for the conversion of PRPn to PRcP by PhnJ is presented in Figure 3.

The reaction intermediates for the conversion of alkyl phosphonates to phosphate in *E. coli* have now been identified. PhnI, in the presence of PhnG, PhnH, and PhnL, catalyzes the formation of RPnTP from MgATP and methylphosphonate. PhnM catalyzes the hydrolysis of RPnTP to pyrophosphate and PRPn. PhnJ can be reconstituted anaerobically with an iron

sulfur center using ferrous sulfate, sodium sulfide and sodium dithionite. The reconstituted PhnJ catalyzes the SAM-dependent radical cleavage of the C-P bond of PRPn to form PRcP and methane. The transformations catalyzed by the C-P lyase system in *E. coli* are summarized in Figure 4.

METHODS SUMMARY

Protein expression and purification

All vectors bearing the appropriate genes were transformed in BL21 DE3 cells and inoculated into LB media. Cells were grown at 37 °C to an A_{600} ~ 0.4, after which the temperature was reduced to 18 °C. At A_{600} ~ 0.6, the cells were induced with 0.5 mM IPTG. Cells were grown for 18–20 hours after induction. Over-expression was confirmed by SDS-PAGE. Detailed descriptions of the protein purification protocols are presented in Supplementary Information. All GST-tagged proteins (PhnI, PhnJ, PhnK and PhnL) were purified on a GSTrap column (GE Healthcare, 5 mL) and all poly-His tag proteins (PhnG and PhnH) were purified on a HisTrap column (GE Healthcare, 5 mL) using the manufacturer's instructions. PhnM was purified using gel filtration with a High Load Superdex 200 26/60 prep grade column followed by anion exchange chromatography (ResourceQ, 6 mL). The chemical reconstitution of PhnJ is explained in detail in the Supplementary Information.

Purification of reaction products and NMR spectroscopy

All reactions were filtered by centrifugation through a 10 or 30 kDa membrane (VWR Chemicals) to separate the enzymes from the reaction mixture. The filtrate (0.5 mL) was loaded onto a 1 mL ResourceQ column and eluted with 0.1 M to 1 M ammonium bicarbonate over 20 mL using an AKTA Purifier 10 HPLC. The peak fractions were collected and vacuum dried at 4 °C. The products were analyzed by ^{1}H, ^{13}C and ^{31}P NMR. The samples for ^{31}P NMR (D_2O, 85% H_3PO_4 = δ 0.00) were made in 50 mM HEPES, 10% D_2O, pH 8.5–8.8 (or 6.8 for PhnJ) and analyzed with a Varian Unity Inova 500 MHz NMR or a Bruker Avance III 400 MHz NMR. ^{1}H and ^{13}C NMR spectra were acquired on a Bruker Avance III 500 MHz NMR equipped with an H-C-N cryoprobe.

Supplementary Material

Refer to Web version on PubMed Central for supplementary material.

Acknowledgments

We thank Professor David Barondeau and his laboratory for use of the anaerobic chamber and for advice on the assembly of iron-sulfur centers in radical SAM enzymes. We also thank Dr. Chengfu Xu for help with some of the ^{31}P NMR spectra and Ms. Samantha Burrows for help with cloning *phnI* and *phnH.* This work was supported in part by the National Institutes of Health (GM93342, GM71790) and the Robert A. Welch Foundation (A-840). The cryoprobe for the NMR was purchased with funds from the National Science Foundation (0840464)

References

1. Metcalf WW, Wanner BL. Evidence for a fourteen-gene, *phnC* to *phnP* locus for phosphonate metabolism in *Escherichia coli*. Gene. 1993; 129:27–32. [PubMed: 8335257]

2. Ahn Y, Ye Q, Cho H, Walsh CT, Floss HG. Stereochemistry of carbon-phosphorus cleavage in ethylphosphonate catalyzed by C-P lyase from *Escherichia coli*. J Am Chem Soc. 1992; 114:7953–7954.
3. Metcalf WW, Wanner BL. Mutational analysis of an *Escherichia coli* fourteen-gene operon for phosphonate degradation, using Tnpho*A'* elements. J Bacteriol. 1993; 175:3430–3442. [PubMed: 8388873]
4. Hove-Jensen B, Rosenkrantz TJ, Haldimann A, Wanner BL. *Escherichia coli phnN*, encoding ribose 1,5-bisphosphokinase activity (phosphoribosyl diphosphate forming): dual role in phosphonate degradation and NAD biosynthesis pathways. J Bacteriol. 2003; 185:2793–2801. [PubMed: 12700258]
5. Errey JC, Blanchard JS. Functional annotation and kinetic characterization of PhnO from *Salmonella enterica*. Biochemistry. 2006; 45:3033–3039. [PubMed: 16503658]
6. Hove-Jensen B, McSorley FR, Zechel DL. Physiological role of *phnP*-specified phosphoribosyl cyclic phosphodiesterase in catabolism of organophosphoric acids by the carbon-phosphorus lyase pathway. J Am Chem Soc. 2011; 133:3617–3624. [PubMed: 21341651]
7. Ternan NG, McGrath JW, McMullan G, Quinn JP. Organophosphonates: occurrence, synthesis and biodegradation by microorganisms. World J Microbio & Biotech. 1998; 14:635–647.
8. Kononova SV, Nesmeyanova MA. Phosphonates and their degradation by microorganisms. Biochemistry (Moscow). 2002; 67:184–192. [PubMed: 11952414]
9. White AK, Metcalf WW. Microbial metabolism of reduced phosphorus compounds. Annu Rev Microbiol. 2007; 61:379–400. [PubMed: 18035609]
10. Avila LZ, Draths KM, Frost JW. Metabolites associated with organophosphonate C-P bond cleavage: chemical synthesis and microbial degradation of [^{32}P]-ethylphosphonic acid. Bioorg & Med Chem Lett. 1991; 1:51–54.
11. Frost JW, Loo S, Cordeiro ML, Li D. Radical-based dephosphorylation and organophosphonate biodegradation. J Am Chem Soc. 1987; 109:2166–2171.
12. Parker GF, Higgins TP, Hawkes T, Robson RL. *Rhizobium (Sinorhizobium) meliloti phn* genes: characterization and identification of their protein products. J Bacteriol. 1999; 181:389–395. [PubMed: 9882650]
13. Kamat SS, et al. Catalytic mechanism and three-dimensional structure of adenine deaminase. Biochemistry. 2011; 50:1917–1927. [PubMed: 21247091]
14. Maynes JT, Yuan RG, Snyder FF. Identification, expression and characterization of the *Escherichia coli* guanine deaminase. J Bacteriol. 2000; 182:4658–4660. [PubMed: 10913105]
15. Hall RS, et al. Three dimensional structure and catalytic mechanism of cytosine deaminase. Biochemistry. 2011; 50:5077–5085. [PubMed: 21545144]
16. Krenitsky TA, Neil SM, Elion GB, Hitchings GH. A comparison of the specificities of xanthine oxidase and aldehyde oxidase. Arch Biochem Biophys. 1972; 150:585–599. [PubMed: 5044040]
17. La Vallie ER, et al. Enzymatic cleavage of fusion proteins with Factor Xa. Curr Protoc Mol Biol. 1994; 2:16.4.6–16.4.7.
18. Jochimsen B, et al. Five phosphonate operon gene products as components of a multi-enzyme complex of the carbon-phosphorus lyase pathway. PNAS. 2011; 108:11393–11398. [PubMed: 21705661]
19. Seibert CM, Raushel FM. Structural and catalytic diversity within the amidohydrolase superfamily. Biochemistry. 2005; 44:6383–6391. [PubMed: 15850372]
20. Frey PA, Hegeman AD, Ruzicka FJ. The radical SAM superfamily. Crit Rev Biochem Mol Biol. 2008; 43:63–88. [PubMed: 18307109]
21. Chatterjee A, et al. Reconstitution of ThiC in thiamine pyrimidine biosynthesis expands the radical SAM superfamily. Nature Chem Biol. 2008; 4:758–765. [PubMed: 18953358]
22. McGlynn SE, et al. Identification and characterization of a novel member of the radical AdoMet enzyme superfamily and implications for the biosynthesis of the Hmd hydrogenase active site cofactor. J Bacteriol. 2010; 192:595–598. [PubMed: 19897660]
23. Zhang Y, et al. Diphthamide biosynthesis requires an organic radical generated by iron-sulphur enzyme. Nature. 2010; 465:891–896. [PubMed: 20559380]

24. Parast CV, Wong KK, Lewisch SA, Kozarich JW. Hydrogen exchange of the glycyl radical of pyruvate formate-lyase is catalyzed by cysteine 419. Biochemistry. 1995; 34:2393–2399. [PubMed: 7873518]

25. Buis JM, Broderick JB. Pyruvate formate-lyase activating enzyme: elucidation of a novel mechanism for glycyl radical formation. Arch Biochem Biophys. 2005; 433:288–296. [PubMed: 15581584]

26. Thauer RK, Shima S. Methane as fuel for anaerobic microorganisms. Ann N Y Acad Sci. 2008; 1125:158–170. [PubMed: 18096853]

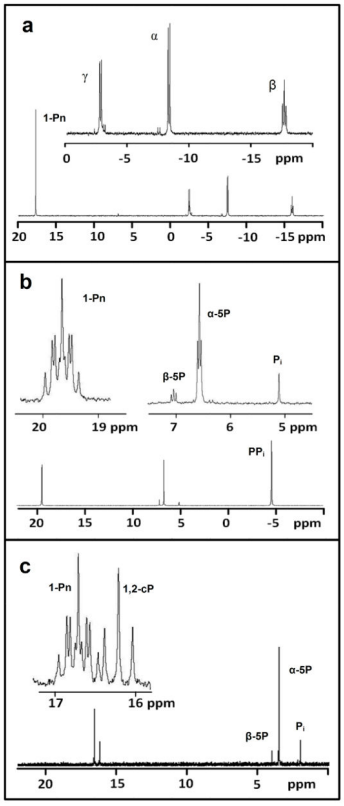

Figure 1. ^{31}P-NMR spectra of the reaction products catalyzed by PhnI, PhnM, and PhnJ

a, RPnTP from the reaction of methyl phosphonate and MgATP catalyzed by PhnI in the presence of PhnG, PhnH, and PhnL at pH 8.5. The inset shows the ^{31}P-^{31}P coupling of the triphosphate portion of the RPnTP product. **b**, The formation of PRPn from RPnTP in the presence of PhnM. The inset displays the proton coupled spectrum at pH 8.5 showing the multiplet that corresponds to the 1-phosphonylmethane and the triplet that corresponds to the 5-phosphate. **c**, The formation of PRcP from PRPn in the presence of PhnJ at pH 6.8. The inset displays the proton coupled spectrum showing the formation of a new triplet that corresponds to the 1,2-cyclic moiety of PRcP. The chemical shifts for the phosphate moiety at C5 of PRcP and PRPn are coincident with one another (3.4 ppm).

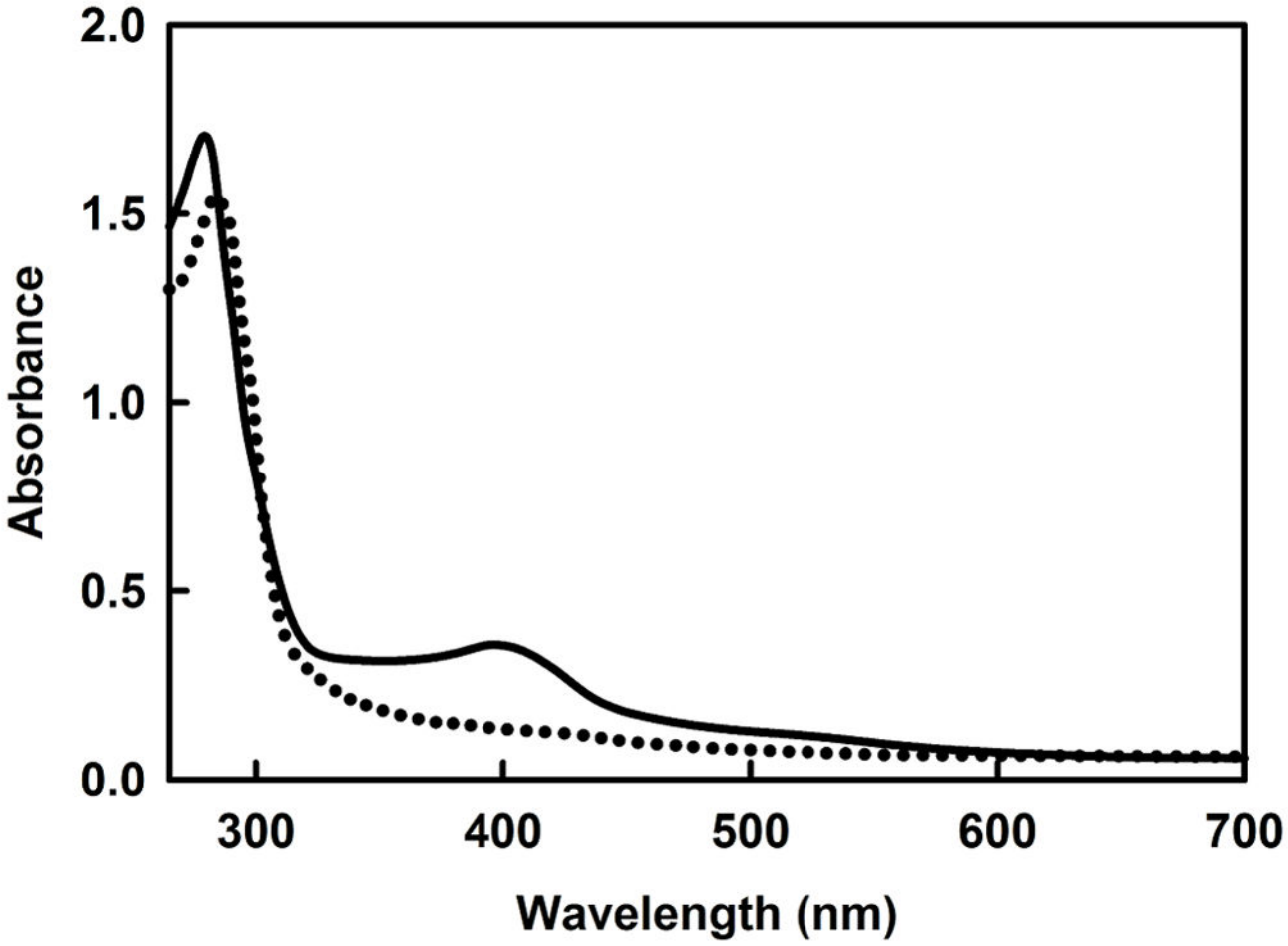

Figure 2. UV-visible absorbance spectrum of PhnJ (31 μM) after anaerobic reconstitution of the iron-sulfur cluster

The peak at 280 nm for the solid line is due to the protein and the absorbance centered at 403 nm represents the $[4Fe\text{-}4S]^{2+}$ cluster. The dotted line represents the absorbance spectrum of PhnJ (27 μM) reconstituted with a $[4Fe\text{-}4S]^{2+}$ cluster after reduction of the cluster with sodium dithionite to the $[4Fe\text{-}4S]^{1+}$ form.

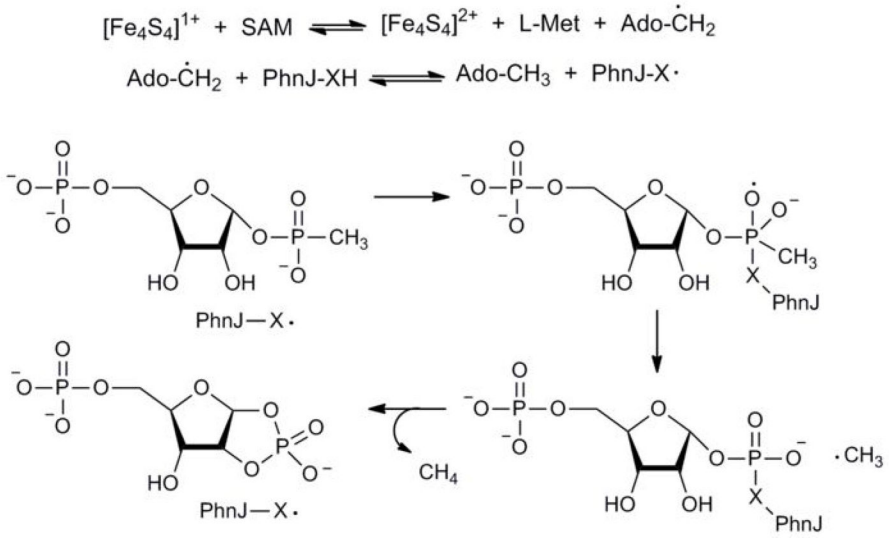

Figure 3. Working model for the transformation of PRPn to PRcP

The cleavage of the C-P bond in PRPn by PhnJ reconstituted with a $[4Fe\text{-}4S]^{1+}$ cluster and SAM is likely initiated via an electron transfer from the iron-sulfur cluster to reductively cleave SAM to transiently generate L-methionine and a 5′-deoxyadenosyl radical. The 5′-deoxyadenosyl radical may subsequently catalyze the formation of a protein radical, presumably a cysteine-based thiyl radical. Thiyl radicals have previously been demonstrated in pyruvate-formate lyase[24, 25] and methyl-coenzyme M reductase[26]. The thiyl radical may attack the phosphonate moiety of the substrate to liberate a methyl radical with formation of a thioester intermediate. Intramolecular attack by the C2 hydroxyl of the substrate would generate PRcP and the free thiol group. Methane would be formed via hydrogen atom abstraction from either 5-deoxyadenosine or the putative cysteine residue.

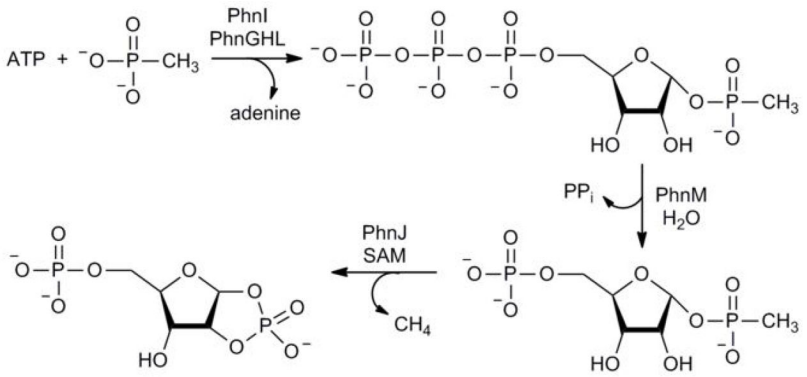

Figure 4. Reaction pathway for the conversion of methyl phosphonate to PRcP

The proteins PhnG, PhnH, PhnI, PhnJ, PhnL, and PhnM are required for this transformation. The role of PhnK is unknown.